Cobalt-Rich Ferromanganese Oxyhydroxide Crusts in the Global Ocean

HEIN, JAMES R., U.S. Geological Survey, MS 999, 345 Middlefield Rd., Menlo Park, CA, 94025, USA

Summary

Co-rich Fe-Mn crusts are a potential resource for Co, Ni, Pt, Mn, Tl, Te, Ti, and other metals. They occur on topographic highs at depths of 400-4000 m throughout the ocean basins where currents have swept the rocks clean of sediment for millions of years. Crusts precipitate from cold ambient seawater as pavements up to 25 cm thick. Gravity processes, sedimentation, reefs, and currents control crust distribution and thickness. Crust layers show massive, botryoidal, laminated, columnar, or mottled textures. Distinct layering sequences are regionally persistent. Most crusts grow at rates of 1-6 mm/Ma and are composed of δ-MnO_2, Fe oxyhydroxide, and minor quartz and feldspar, with carbonate fluorapatite (CFA) in thick (>6 cm) crusts. Elements associated with δ-MnO_2 include Co, Ni, Cd, Tl, Te, and Mo, and with Fe oxyhydroxide, As. Co contents are as high as 2.3%, Ni to 1%, and Pt to 3 ppm, with mean Fe/Mn ratios of 0.7-1.5. Co, Ni, Ti, and Pt are greater in central-Pacific crusts, whereas Fe/Mn, Si, and Al are greater in continental margin, Atlantic, and Indian crusts. Total REEs vary from 0.1 to 0.3% and are derived from seawater, as are Co, Mn, Ni, Tl, and most Pt-group elements. Co, Ce, Tl, and possibly also Ti, Pb, Te, and Pt are more concentrated in crusts than other metals because of oxidation reactions. Other controls on element abundances in crusts include the concentration of metals in seawater, colloid surface charge, complexing agents, surface area, growth rates, and bacterially mediated reactions.

Introduction

Fe-Mn oxyhydroxide crusts are ubiquitous on hard-rock substrates throughout the ocean basins. They form on the flanks and summits of seamounts, ridges, plateaus, and abyssal hills where the rocks have been swept clean of sediments at least intermittently for millions of years. Crusts form pavements up to 25 cm thick on rock outcrops, or coat talus debris. Crusts form by hydrogenetic precipitation from cold ambient bottom waters, or by a combination of hydrogenetic and hydrothermal precipitation in areas of hydrothermal venting.

Distribution

Fe-Mn crusts occur on Pacific seamounts as far north as the Aleutian Trench and as far south as the Circum-Antarctic Ridge. Compared to the estimated 50,000 or so seamounts in the Pacific, the Atlantic and Indian oceans contain fewer seamounts and most crusts are associated with spreading ridges. Those crusts usually have a hydrothermal component that may be large near active venting, but which is regionally generally a small (<30%) component of the crusts formed along most of the ridges (Bury, 1989). Fe-Mn crusts occur at water depths of about 400-4000 m, but most commonly occur at depths from about 1000-3000 m. The most Co-rich crusts occur at water depths from 800-2200 m, which mostly encompasses the OMZ. The thickest crusts occur at depths of 1500-2500 m, which corresponds to depths of the outer summit area and upper flanks of most Cretaceous seamounts.

Textures and Physical Properties

Crust surfaces exposed directly to the seafloor are botryoidal, with botryoids varying in size from a mm to several cm. Under conditions of high current flow, botryoids are modified, either by smoothing or by accentuation of the relief by erosion around botryoid margins, in places producing mushroom-shaped forms. Strong uni-directional flow polishes and flutes botryoids. Crust profiles vary according to crust thickness and oceanographic conditions. The thickest crusts (>80 mm) may have up to 8 distinct macroscopic layers, the lower layers of which may be phosphatized. Thick crusts typically have 4-5 macroscopic layers that are consistent regionally.

An important consideration for the exploration and exploitation of potential crust resources is their contrast in physical properties with substrate rocks. Those comparisons are complicated by the fact that crusts grow on a variety of substrate types including breccia, basalt, phosphorite, limestone, hyaloclastite, and mudstone. Fresh basalt and phosphorite contrast significantly with crusts, whereas the other rock types and altered basalt may not contrast in physical properties with crusts. Crusts are generally much more porous (mean 60%) than substrate rocks and have extreme specific surface areas, averaging 300 m^2/g. The P-wave velocity of crusts may be less or more than that of sedimentary substrate rocks, but is generally less than that of basalt. This variable contrast makes it difficult to develop sonic devices for measuring *in situ* crust thicknesses. The most distinctive property of crusts is their gamma radiation, which averages 475 net counts/min, in contrast to sedimentary rock (101) and basalt (146) substrates (Svininnikov, 1994). Gamma radiation may be useful for crust exploration under thin sediment cover and for measuring crust thicknesses *in situ*.

Mineralogy, Growth Rates, and Ages

The dominant crystalline phase is Fe-rich δ-MnO_2, (ferruginous vernadite), which generally makes up more than 95% of the crystalline phases, the remainder being detrital minerals. The older parts of thick crusts are phosphatized and may contain up to 30% CFA in that part of the crust, but CFA is generally less than 10% of thick bulk crusts. Another major phase in crusts is X-ray amorphous Fe oxyhydroxide (δ-FeOOH, feroxyhyte), which is epitaxially intergrown with δ-MnO_2. Todorokite, common in diagenetic Fe-Mn nodules and hydrothermal Mn deposits, is rare in hydrogenetic crusts--only 5% of 640 crust analyzes showed the presence of todorokite.

Hydrogenetic Fe-Mn crusts grow at incredibly slow rates of <1 to about 10 mm/Ma, with the most common rates being from 1-6 mm/Ma. These slow growth rates allow for the adsorption of large quantities of trace metals by the oxyhydroxides at the crust surface. The initiation of growth of the thickest crusts began about 60 Ma ago.

Chemical Composition

USGS chemical data presented here (Table 1, columns 1-5, 8-10, 13-14) are normalized to 0% H_2O^- because hygroscopic water varies markedly up to 30 wt.%, thereby affecting the contents of all the elements. Unfortunately, water contents are not provided in many papers, so we were unable to correct compiled data listed in Table 1 (columns 6, 7, 11, 12, 15, 1--sources are listed in Hein *et al.* (1999)). Mean chemical compositions are provided for crusts that occur in the areas marked on Fig. 1 as well as for

Atlantic and Indian crusts, all of which correspond to columns in Table 1. Hydrogenetic crusts generally have Fe/Mn ratios between 0.4 and 1.2, most commonly 0.7±0.2, whereas mixed hydrogenetic and hydrothermal crusts and continental margin crusts have ratios between 1 and 3, mostly 1.3-1.8 (Table 1). Co, the metal of greatest economic potential, ranges from about 0.1-2.3% in bulk crusts and averages from 0.2% to 0.7% for various regions of the global ocean (Table 1). Co is also considered the element most characteristic of hydrogenetic precipitation in crusts and is considered to maintain a constant flux in the oceans, regardless of water depth (Halbach *et al.*, 1983). Based on sequential leaching experiments, Koschinsky and Halbach (1995) provided the following list of elements with decreasing degrees of hydrogenesis: Co=Mn>Ni>Zn=Pb=Cu>Fe>Ti. Ni and Pt are also considered of economic importance and range up to 1.0% and 1 ppm respectively for bulk crusts. Pt ranges up to 3 ppm for individual crust layers. Elements most strongly enriched over abyssal Fe-Mn nodules include Co, Pt, Pb, V, P, Ca, Ti, Sr, Te, and REEs, whereas nodules are more enriched in Cu, Ni, Zn, Al, K, and Cd. Crusts are enriched over lithospheric contents about 30,000 times for Te and 100 to 500 times for Mo, Tl, Sb, Co, Mn, Bi, As, Se, and Pb.

Elements in crusts have different origins and are associated with different crust mineral phases. Mn, Co, Ni, Cd, and Mo are invariably associated with the δ-MnO_2 phase and Pb, V, Zn, Na, Ca, Sr, Mg, and Ti are associated with that phase in some regions. Fe and As are usually the only elements associated with the Fe oxyhydroxide phase, although V, Cu, Pb, Y, P, Cr, Be, Sr, Ti, and Ce are also associated with that phase in some regions. The detrital phase always includes Si, Al, and K, and commonly also Ti, Cr, Mg, Fe, Na, and Cu. The CFA phase invariably includes Ca, P, and CO_2, and also commonly Sr and Y. The residual biogenic phase usually includes Ba, Sr, Ce, Cu, V, Ca, and Mg. CFA associated elements and Pt, Rh, and Ir generally increase with increasing crust thickness, whereas Co and detrital phase associated elements usually decrease with increasing crust thickness.

Fe-Mn Crust Formation

Even though Fe-Mn crusts form by hydrogenetic precipitation, the exact mechanisms of metal enrichments in the water column and at the crust surface are poorly understood. Elements in seawater may occur in their elemental form or as inorganic and organic complexes. Those complexes may in turn form colloids that interact with each other and with other dissolved metals. Thermodynamic, surface-chemical, and colloidal-chemical models show that most hydrogenetic elements in crusts occur as inorganic complexes in seawater. Hydrated cations (Co, Ni, Zn, Pb, Cd, Tl, etc.) are attracted to the negatively charged surface of Mn oxyhydroxide, whereas anions and elements that form large complexes with low charge-density (V, As, P, Zr, Hf, etc.) are attracted to the slightly positive charge of Fe oxyhydroxide surfaces (Koschinsky and Halbach, 1995).

Mixed Fe and Mn colloids with adsorbed metals precipitate onto hard-rock surfaces as poorly crystalline or amorphous oxyhydroxides, probably through bacterially mediated catalytic processes. Continued crust accretion after precipitation of that first molecular layer is autocatalytic, but is probably enhanced to some degree by bacterial processes. Additional metals are incorporated into the deposits either by co-precipitation, or by diffusion of adsorbed ions into the Mn and Fe oxyhydroxide crystal lattices. Co is highly enriched in crusts because it is oxidized from Co^{2+} to the less soluble Co^{3+} at the crust surface, possibly through a disproportionation reaction. Pb, Ti, Ce, and Tl, are also highly enriched in hydrogenetic deposits, probably by a similar oxidation mechanism. Concentrations of elements in seawater are generally reflected in their concentrations in crusts, although many mitigating factors exist. For example, Cu, Ni, and Zn occur in comparable concentrations in seawater, yet Ni is much more enriched in crusts than either Cu or Zn. However, comparable proportions of Mn:Fe:Co exist in deep seawater (0.5-1.0:1:0.02-0.05) as exist in crusts (0.6-1.6:1:0.02-0.05; Table 1).

The dominant controls on the concentration of elements in crusts are the concentration of each element in seawater; element-particle reactivity--residence times in seawater; the absolute and relative amounts of Fe and Mn in the crusts, which in turn are related to their abundance and ratio in colloidal flocs in seawater (Aplin and Cronan, 1985); the colloid surface charge and types of complexing agents, which will determine the amount of scavenging within the water column; the degree of oxidation of MnO_2 (O/Mn)--the greater the oxidation the greater the adsorption capacity (Gramm-Osipov et al., 1994); the amount of surface area available for accretion, which at the surface of growing crusts is extremely large, but which decreases with maturation of the crusts; the amount of dilution by detrital minerals and diagenetic phases; and growth rates. Accretion of oxyhydroxides will be slower where the OMZ intersects the seafloor than it will be above and below that zone, because Mn is more soluble in low-oxygen seawater. Crusts exposed at the seafloor may not necessarily be actively accreting oxyhydroxides because of mechanical erosion or, less commonly in the contemporary oceans, because of seawater oxygen contents that are insufficient to permit oxidation of the major metals.

References

Aplin, A. C., and Cronan, D. S., 1985. Ferromanganese oxide deposits from the central Pacific Ocean, I. Encrustations from the Line Islands Archipelago. Geochimica et Cosmochimica Acta, 49: 427-436.

Bury, S. J., 1989. The geochemistry of North Atlantic ferromanganese encrustations. Ph.D. Thesis, Cambridge University, 265 pp.

Gramm-Osipov, L. M., Hein, J. R., and Chichkin, R. V., 1994. Manganese geochemistry in the Karin Ridge region: Preliminary physiochemical description. U.S. Geological Survey Open File Report 94-230: 99-102.

Halbach, P., Segl, M., Puteanus, D., and Mangini, A., 1983. Co-fluxes and growth rates in ferromanganese deposits from central Pacific seamount areas. Nature, 304: 716-719.

Hein, J. R., Koschinsky, A., Bau, M., Manheim, F. T., Kang, J.-K., and Roberts, L., 1999. Cobalt-rich ferromanganese crusts in the Pacific. In: Cronan, D.S. (Ed.) Handbook of Marine Minerals. CRC Press, p. 239-279, Boca Raton, Florida.

Koschinsky, A. and Halbach, P., 1995. Sequential leaching of ferromanganese precipitates: Genetic implications. Geochimica et Cosmochimica Acta, 59: 5113-5132.

Sviniinnikov, A. I., 1994. Physical properties of rocks and sediments from Karin Ridge (Central Equatorial Pacific) and the Bering Sea. U.S. Geological Survey Open File Report 94-230: 103-118.

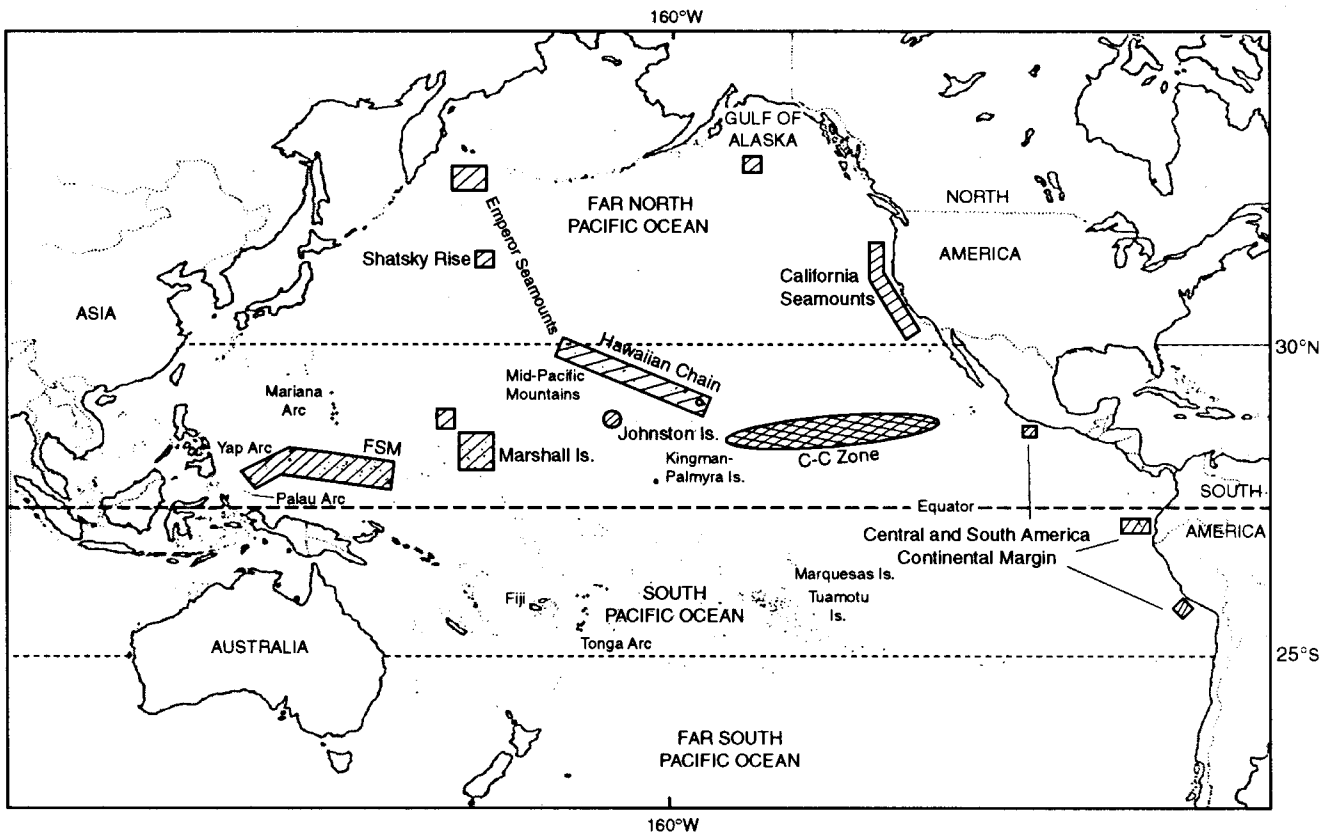

Figure 1. Lined boxes are areas with mean Fe-Mn crust compositional data listed in Table 1. The far North Pacific data are from the two indicated boxes, whereas the far South Pacific data covers areas mostly offshore New Zealand and southern Australia; the south Pacific data span most of the area between South America and the West Pacific arcs and between the equator and 25° south latitude; the cross-hatched oval area is the Clarion-Clipperton prime Fe-Mn nodule zone.

Table 1. Mean chemical composition of Fe-Mn crusts from various parts of the Pacific, Indian, and Atlantic Oceans

	FSM-Palau n=35	Marshall Is. n=116	NW of Marshall Is. n=43	Johnston I. n=103	Calif. Border-land n=71	NW Pacific n=1478	Hawaii n=205	Far North Pacific n=6	Shatsky Rise n=20	C&S Am. Cont Margin n=6	South Pacific 0-25° Lat n=228	Far South Pacific >25° Lat n=51	Atlantic n=25	Indian n=14	C-C Zone Nodules n=100-4000	Other Abyssal Nodules n=100-4000
Fe/Mn	0.82	0.67	0.76	0.71	1.24	0.68	1.17	0.95	0.93	1.07	0.98	1.14	1.54	1.52	0.27	0.69
Fe wt. %	20.3	15.7	16.6	17.4	19.5	15.1	20.6	20.3	22.5	25.9	21.2 (193)	19.0	21.6	23.6	6.9	12.7
Mn	24.9	23.3	21.7	24.4	15.7	22.1	17.6	21.4	24.3	24.1	21.6	16.7	14.0	15.6	25.4	18.5
Si	5.50	2.80	5.38	4.06	10.5	3.7 (273)	7.29 (114)	4.52	9.45	8.28	4.28 (178)	7.14 (34)	5.50	7.78	7.6	8.8
Na	2.14	1.57	1.70	1.67	1.81	1.6 (175)	1.61 (114)	2.04	1.92	1.85	1.76 (25)	0.88 (21)	2.16	2.24	2.8	2.1
Al	1.31 (34)	0.63	1.15	0.81	1.95	1.0 (328)	2.46 (194)	1.02	1.97	2.10	1.30 (192)	3.55 (7)	1.54	1.34	2.9	3.0
K	0.55	0.47	0.64	0.55	0.80	0.56 (177)	0.64 (114)	0.49	0.97	0.81	0.54 (93)	0.35 (18)	4.39	2.32	1.0	0.93
Mg	1.15	1.05	1.02	1.08	1.14	1.3 (342)	1.15 (171)	1.14	1.60	1.36	1.31 (143)	1.36 (7)	1.32	1.72	1.7	1.4
Ca	2.76	5.86	3.57	3.17	1.77	4.1 (374)	2.29 (171)	2.72	2.61	2.81	2.70 (192)	2.22 (18)	0.53	0.75	1.7	1.8
Ti	1.010	1.014	1.137	1.216	0.550	0.77 (370)	1.673 (188)	0.846	1.001	1.029	1.073 (181)	0.738 (7)	0.948	1.015	0.53	0.78
P	0.47	1.64	0.77	0.61	0.37	1.2 (332)	0.40 (171)	0.49	0.55	0.54	0.63 (180)	0.45 (34)	0.78	0.38	0.10A	0.10A
Cl	0.95 (6)	0.92 (40)	0.77 (1)	0.86 (2)	0.85 (4)	--	--	1.07 (3)	1.11 (20)	1.04 (6)	1.41 (6)	--	1.02 (13)	1.38 (10)	--	--
H_2O^+	9.3 (29)	7.6 (76)	8.4	8.5	9.21 (69)	--	8.3 (100)	--	--	--	10.2 (7)	--	28.3	26.2	7.5A	7.5A
H_2O^-	17.2	19.2	24.5	20.4	21.3	--	12.3 (95)	14.7	18.0	18.6	18.5 (13)	--	11.2	12.8	--	--
Ag ppm	--	--	--	--	--	0.717 (32)	--	--	10.2 (1)	--	--	--	--	--	0.10A	0.10A
As	272 (31)	212	234	258	230	165 (106)	246 (171)	259	210	246	254 (28)	544 (14)	289 (24)	181 (10)	159A	159A
B	238 (6)	179 (40)	177 (1)	162 (2)	315 (4)	115 (37)	--	278 (3)	326	381	336 (6)	--	257 (13)	287 (10)	273A	273A
Ba	1547	1987	2018	1865	3285	1695 (266)	1616 (171)	1844	2646	2150	1745 (86)	1298 (13)	1716	1668	2800	2000
Bi	17.5 (6)	41.0 (31)	59.1 (1)	64.3 (2)	9.5 (4)	--	--	30.7 (4)	33.3	12.7	25.4 (6)	--	15.3 (20)	16.9 (13)	21A	21A
Ce	800 (29)	1072 (76)	1286	1229	1050 (69)	1105 (48)	1911 (114)	--	--	--	592 (3)	--	--	--	530A	530A
Co	3910	6410	5019	7441	2746	6372(1440)	4156 (205)	4349	2713	1918	5508	3878 (50)	3574	3126	2400	2400
Cr	31 (31)	24 (104)	17 (42)	8 (95)	31	22.4 (67)	48.1 (83)	31 (3)	33	67	35 (17)	34 (9)	31 (22)	33 (9)	27	25
Cu	878	963	1310	1059	679	1075(1418)	999	298	1270	558	1100	761	774	1254	10200	4200
Ga	30 (6)	19 (31)	--	11 (2)	16 (4)	--	--	11 (4)	13	27	18 (6)	--	16 (21)	18	11A	11A
Hf	7 (2)	10 (40)	7 (1)	7 (2)	7 (4)	7.4 (6)	--	7 (3)	5 (18)	8	7 (25)	8 (11)	14 (12)	10 (7)	6A	6A
Li	5 (6)	3 (30)	4 (1)	2 (2)	12 (4)	63 (2)	--	5 (4)	12	6 (5)	4 (6)	--	35 (24)	10 (13)	160A	160A
Mo	403	504	420	482	329	455 (172)	232 (171)	794	530	471	470 (27)	--	429	330	520	360
Nb	54 (6)	51 (40)	70 (1)	48 (2)	32 (4)	--	--	34 (5)	43	40	62 (6)	--	54	74	74A	74A
Ni	3495	4626	3927	4398	2926	5403(1427)	2337	3393	3241	2654	4237 (214)	3385	2685	2558	12800	6300
Pb	1329	1505	1713	1723	1207	1777 (307)	1537 (170)	1746	1740	833	1207 (46)	1531 (24)	1108	1058	450	820
Sb	43.3 (2)	38.7 (40)	49.0 (1)	45.1 (2)	44.4 (4)	24.4 (47)	--	48.5 (3)	43.0	30.4	40.3 (19)	28.5 (14)	57.2 (12)	43.1 (6)	37A	37A
Sc	9.4 (6)	6.4 (40)	9.8 (1)	7.9 (2)	10.0 (4)	6.4 (64)	--	9.1	11.7	8.4	8.1 (26)	7.8 (14)	17.3	12.3	10A	10A
Sr	1505	1614	1531	1624	1241	1212 (166)	1267 (114)	1619	1539	1399	1521 (27)	--	1341	1124	450	700
Ta	--	3 (1)	--	1 (1)	18 (1)	--	--	--	4 (16)	2 (2)	3 (2)	--	--	3 (1)	--	--
Te	31.0 (6)	60.8 (40)	46.8 (1)	51.0 (2)	8.7 (4)	--	--	19.6 (4)	25.5	20.9	35.2 (6)	--	37.2 (20)	32.8 (13)	216A	216A
Tl	107 (6)	150 (31)	226 (1)	193 (2)	54.0 (4)	--	--	127.7 (4)	80.0	76.6	190 (6)	--	94.5 (20)	89.4 (13)	169A	169A
Th	11.4 (2)	11.2 (37)	15.9 (1)	13.5 (2)	31.1 (4)	33.0 (12)	--	37.2	55.0	19.4	14.9 (9)	24.8 (14)	51.9 (24)	50.3 (9)	28A	28A
U	12.5 (2)	12.3 (35)	13.7 (1)	13.6 (2)	10.9 (4)	9.6 (2)	--	15.6 (4)	10.8	14.1	13.3 (11)	7.4 (9)	10.2 (17)	9.1 (9)	6.8A	6.8A
V	657	650	638	639	556	515 (163)	561 (171)	768	549	702	710 (137)	--	825	624	470	480
W	102 (2)	88 (33)	135 (1)	72 (2)	69 (4)	93.3 (44)	--	120 (4)	56	65 (3)	110 (5)	43 (11)	77 (17)	78 (9)	76A	76A
Y	196	251 (107)	225	204	159	166 (104)	189 (114)	200	178	195	205 (9)	--	184	163	133A	133A
Zn	659	719	646	697	620	680 (335)	657 (168)	535	674	597	688 (115)	822 (24)	598	533	1400	900
Zr	586 (6)	538 (40)	678 (1)	682 (2)	605 (4)	172 (76)	--	544 (4)	602	570	610 (6)	--	564 (20)	706 (13)	350	620
Au ppb	--	107 (6)	--	57 (1)	26 (2)	--	--	30 (1)	25 (17)	17 (3)	30 (11)	36 (1)	6 (2)	31 (1)	--	--
Pt	217 (15)	489 (37)	510 (18)	220 (24)	69 (15)	777 (113)	155 (3)	157 (1)	259 (9)	117 (5)	286 (10)	--	567 (2)	348 (2)	97A	97A

Pacific areas outlined in Fig. 1; dash means not analyzed; n in parentheses differ from those in heading; A = means for the entire Pacific